Enhancing electron mobility at the $LaAlO_3/SrTiO_3$ interface by surface control

By *Yanwu Xie, Christopher Bell, Yasuyuki Hikita, Satoshi Harashima and Harold Y. Hwang*

[*] Dr. Y. W. Xie, Prof. H. Y. Hwang
Geballe Laboratory for Advanced Materials, Department of Applied Physics, Stanford University, Stanford, California 94305, USA

Dr. Y. W. Xie, Dr. C. Bell, Dr. Y. Hikita, S. Harashima, Prof. H. Y. Hwang
Stanford Institute for Materials and Energy Sciences, SLAC National Accelerator Laboratory, Menlo Park, California 94025, USA

S. Harashima
Department of Applied Physics, The University of Tokyo, Bunkyo-ku, Tokyo 113-8656, Japan
Email: xieyanwu@stanford.edu

Keywords: $LaAlO_3/SrTiO_3$, interface, surface charge, adsorbate

The fascinating quantum properties of $SrTiO_3$ at low temperatures, in particular the low carrier density superconductivity[1] and the extremely large dielectric constant (exceeding 20,000 at a temperature T = 2 K)[2] make this system rather distinct from that of conventional semiconductors. Among the various routes to establish a novel two-dimensional electron gas in $SrTiO_3$, the interface between the two band insulators $LaAlO_3$ and $SrTiO_3$ has attracted the most significant research interest,[3] since metal-insulator transitions,[4,5] low dimensional superconductivity,[6] magnetism,[7] and even their coexistence[8,9,10] have been reported in this system. However, despite intense studies, methods to enhance the electron mobility, μ, of this system have been somewhat limited, hindering progress to enter a regime where quantum phenomenon can be investigated in detail. Here, we demonstrate a strategy to flexibly tune μ using a combination of surface degrees of freedom, building on our previous studies of charge writing using conducting atomic force microscopy (CAFM),[11] and surface adsorption of polar chemical solvents.[12] We demonstrate highly effective tuning of the sheet carrier density, n_{sheet}, with concomitant variation in μ, which increases monotonically with the decrease of

Work supported by US Department of Energy contract DE-AC02-76SF00515 and BES.

n_{sheet} over a wide range. By optimizing the surface preparation, we could enhance μ as high as 20,200 $cm^2V^{-1}s^{-1}$, three times the maximum value reported previously.[13]

Although the conventional field effect configuration through the $SrTiO_3$ has been used very successfully to tune n_{sheet} and the electronic ground state of the interface electrons,[4, 6,14,15] the strong suppression of μ as n_{sheet} is decreased using back-gating[14] prevented the observation of quantum transport in the relatively low density limit. Only very recently have samples with $n_{sheet} < 10^{13}$ cm^{-2}, and sufficiently high μ to observe Shubnikov-de Haas oscillations become accessible.[13, 16] These improvements were achieved either by decreasing the growth temperature[13] or using capping layers,[16] with a maximum reported μ of 6,600 $cm^2V^{-1}s^{-1}$.[13] However, further improvements in μ are essential, and it is therefore vital to consider additional techniques beyond growth variation, to enhance device flexibility.

In this context, the strong surface-interface coupling in the $LaAlO_3/SrTiO_3$ heterostructure[17] provides a unique way to control the interfacial electrons from the $LaAlO_3$ surface via charges[5,11,18-20] or adsorbates.[12] Previously, we have demonstrated that surface charges can increase or decrease n_{sheet}, depending on their polarity,[11] and that the adsorption of molecules on the $LaAlO_3$ surface also strongly increases n_{sheet}, to a degree that scales with the molecular dipole density.[12] Using either technique, the change in n_{sheet} could be as large as 1×10^{13} cm^{-2}, comparable to the tuning range with the electric field effect.[4,14,15] Thus we have two powerful ways to tune n_{sheet} from the sample surface, with a third level of control provided by heating in an intermediate temperature range sufficient to distribute the charges, or remove surface adsorbates without significantly changing the atomic structure of the samples. In this work, we will discuss how these approaches have been combined to enhance μ above 20,000 $cm^2V^{-1}s^{-1}$ for n_{sheet} as low as 1.5×10^{12} cm^{-2}.

Figure 1 shows a typical CAFM tuning on a sample grown under similar conditions to those used by Caviglia *et al.*[13] where two-dimensional quantum oscillations of the longitudinal resistance were measured at low temperatures. As described previously,[11,18]

charges were deposited on the surface of $LaAlO_3$ using a biased CAFM probe. As shown in Figure 1a, positive charge ($V_{tip} > 0$) increases n_{sheet} over a wide temperature range 2 K ≤ T ≤ 300 K, while for $V_{tip} < 0$ (negative deposited charge) n_{sheet} decreases. Note that in our previous report,[11] utilizing different growth conditions, the contrast in transport properties between $V_{tip} < 0$ and $V_{tip} > 0$ was unclear below 100 K. Here we stress that the changes in the sample properties are clearly demarked over the entire temperature range. In Figure 1b we present $\mu(T)$ for the same tuned sample. At low temperatures, where phonon scattering is suppressed,[21, 22] μ is significantly different for the three cases. Notably, at T = 2 K, for $V_{tip} <$ 0, μ increases from 3,800 to 6,500 $cm^2V^{-1}s^{-1}$, while the positive treatment decreases it to less than 2,600 $cm^2V^{-1}s^{-1}$. These initial observations already suggest that using the CAFM treatment μ scales inversely with n_{sheet}, in rather a similar way to electron-doped bulk $SrTiO_3$.[22]

Next, we show typical tuning results by surface exposure to polar solvents followed by heating. Here we use water as the solvent, as described in the experimental section. As shown in **Figure 2a** and its inset, the adsorption of water on the $LaAlO_3$ surface significantly decreases (increases) R_{sheet} (n_{sheet}) (from labels 1 to 2). Subsequent heating in oxygen progressively desorbs the adsorbates and the carrier density is tuned accordingly (through labels 3 to 6). Except for the anomalous increase in n_{sheet} for step 5, the data show rather systematic trends. From **Figure 2b** we see two important features. First, as in the tuning by CAFM, μ scales inversely with n_{sheet}. Second, μ is enhanced (above the line) by a low temperature heating (≤ 200 °C) while decreased (below the line) after heating at higher temperatures (≥ 350 °C). In **Figure 2c** we also plot μ as a function of residual resistivity ratio, *RRR*, defined as R_{sheet}(290 K)/R_{sheet}(2 K), and find that μ increases monotonically with the increase of *RRR*.

In order to investigate the scaling of μ with n_{sheet} over a wide range, we have grown samples under a variety of conditions, performed a wide range of CAFM, solvent, and heating

treatments. A summary of these results is given in **Figure 3**, where we include data only for samples which maintained metallic conductivity down to T = 2 K. For comparison, we also plot the data of the high μ samples reported by Caviglia *et al.* [13] and Huijben *et al.*[16] From Figure 3 one can see that by varying the growth conditions the as-grown samples (circles) can have a broad n_{sheet} range from 4×10^{12} to 6×10^{13} cm^{-2}. Starting from this basis, the surface preparation can fine tune the samples, providing a vast array of possible values of n_{sheet}. Despite the large variety in growth conditions and treatments, interestingly, the uniform trend is that μ increases with decreasing n_{sheet}.

In this context we can ask what are the microscopic mechanisms that are limiting μ. In bulk $SrTiO_3$, the low-temperature μ is dominated by residual impurity scattering.[21,22] However, a CAFM or solvent treatment is not expected to significantly change the concentration and distribution of impurities in $SrTiO_3$. Instead, here we have two contributions. The first one is the spatial distribution of the electrons in the direction perpendicular to the interface. The self-consistent confining potential becomes weaker when n_{sheet} is lower, and thus the charge density will spread much deeper into $SrTiO_3$.[14,23,24] The deeper $SrTiO_3$ layer from the interface is cleaner, and thus a relatively higher μ results. The second contribution takes into account the remote scattering from the surface. In an electronic reconstruction picture[17] electrons transfer from the surface of $LaAlO_3$ to the interface, forming the conductive layer, and leaving the positive ions on the $LaAlO_3$ surface. The electrons can be scattered by the screened potential of the surface positive ions, in a manner similar to modulation-doped heterostructures.[25] Assuming that the effective concentration of surface scattering ions is proportional to n_{sheet}, qualitatively the present observations are consistent with this contribution, although further studies are needed to determine which of these mechanisms dominate the mobility. In addition, multiple subbands exist at $LaAlO_3/SrTiO_3$ interfaces.[24, 26, 27] The high μ observed here suggests that the light effective mass subband is predominantly populated in the low n_{sheet} samples.

Inspired by the inverse scaling of μ with n_{sheet}, we have explored high μ samples by intentionally decreasing n_{sheet}. The lowest n_{sheet} we observed in the present work is 1.5×10^{12} cm^{-2} (Figure 3, star symbol), with a corresponding μ of 20,200 $cm^2V^{-1}s^{-1}$, significantly higher than any other confined low-density electrons in $SrTiO_3$ to date. Although this value cannot be simply related to that in the three-dimensional bulk $SrTiO_3$ crystals, we note that it is also comparable to the maximum μ observed in bulk,[20, 28] although less than one bulk film grown by molecular beam epitaxy.[29] It is instructive at this point to clarify the sequence used for this sample. Firstly, we emphasize that CAFM itself can drive the samples fully insulating by reducing n_{sheet}. Due to the decay of surface charge with time[11, 18] and the adsorption of atmospheric water,[12] n_{sheet} gradually increases at room temperature in ambient exposure. In principle, we can tune n_{sheet} continuously from the low density limit over time. However, this process is rather time-consuming, so instead we next heated the sample at 200 °C to facilitate the diffusion of surface charge, and finally used a chloroform surface treatment to slightly increase n_{sheet} and achieve metallic conductivity. The use of the weakly polar solvent is essential to avoid the relatively large increases in n_{sheet} found with water, for example, which overwhelms the effect of the previous CAFM treatment.[12]

In summary, we have tuned the interface electrons at the $LaAlO_3/SrTiO_3$ interface using surface treatments induced by CAFM, solvent, and heating. Our results demonstrate that μ is inversely proportional to n_{sheet} in a general manner for both the as grown and surface treated samples. By the combination of growth and surface control, we could achieve n_{sheet} values as low as 1.5×10^{12} cm^{-2}, with μ > 20,000 $cm^2V^{-1}s^{-1}$. The present study provides a flexible and powerful way in controlling this system, which might be exploited to construct high μ oxide systems that host quantum transport and spin-orbit coupling simultaneously.

Experimental Section

Sample growth. The $LaAlO_3/SrTiO_3$ samples were prepared by growing $LaAlO_3$ thin films on TiO_2 terminated {100} $SrTiO_3$ substrates by pulsed laser deposition. Before growth the $SrTiO_3$ substrate was patterned into Hall bar shapes by conventional optical lithography and lift off of an amorphous AlO_x hard mask [11, 18, 30]. For the various samples, the growth of $LaAlO_3$ was performed at temperatures ranging from 600 to 800 ˚C, in 1.3×10^{-3} to 2.6×10^{-3} Pa of O_2; after a pre-annealing of substrates at 950 ˚C in 6.7×10^{-4} Pa of O_2 for 30 minutes; and followed by a post annealing at a temperature from 500 to 600˚C, in $> 2\times10^4$ Pa of O_2 for 1 hour to remove potential oxygen vacancies in the $SrTiO_3$. The laser fluence at the $LaAlO_3$ target was between 0.6 and 1.0 Jcm^{-2}. The thickness of $LaAlO_3$ films was monitored using *in situ* reflection high-energy electron diffraction.

CAFM. The CAFM treatment was performed using a multimode Digital Instruments NANOSCOPE 3100 AFM system, using Pt/Ir5 coated silicon tips (Arrow NCPT, Nanoworld. Force constant = 40 N/m; resonance frequency = 270 kHz). All experiments were performed in air, at room temperature, with a relative humidity of 20-40%. All writing was performed in tapping-mode with amplitude feedback. The amplitude setpoint was 1-2% of typical values for topographic imaging. Further experimental details can be found elsewhere [11, 18]. In the present study the writing was achieved by scanning the active device area, with a typical tip velocity of 100 μm/s. The typical value of the applied bias to the CAFM tip is from 6 to 8 V. After the CAFM treatment we waited for at least 3 hours before transport measurements to avoid the initial rapid decay of the surface charges [11].

Solvent treatment. For the solvent treatment, a drop of liquid solvent approximately 1 ml in volume was placed on the sample surface at ambient conditions and then removed within less than 10 s using dry nitrogen gas, with no visible solvent remaining on the surface. An extended discussion of the effects of a wide variety of solvents can be found elsewhere [12].

Heating. The heating was carried out inside a quartz tube furnace in a temperature range between 200 and 400 ˚C, in a flow of O_2 at 10^5 Pa, unless otherwise specified.

Transport measurements. All transport measurements were performed using a standard Hall bar configuration with current biases in the range of 1-10 μA. The electrical contacts to the buried metallic layer were made by ultrasonic bonding with Al wires.

Acknowledgements

This work is supported by the Department of Energy, Office of Basic Energy Sciences, under Contract No. DE-AC02-76SF00515. Y.W.X. also acknowledges partial funding from the AFOSR-MURI on "Quantum Preservation, Simulation & Transfer in Oxide Nanostructures".

Received: ((will be filled in by the editorial staff))
Revised: ((will be filled in by the editorial staff))
Published online: ((will be filled in by the editorial staff))

[1] J. F. Schooley, W. R. Hosler, M. L. Cohen, *Phys. Rev. Lett.* **1964**, *12*, 474.
[2] T. Sakudo, H. Unoki, *Phys. Rev. Lett.* **1971**, *26*, 851.
[3] A. Ohtomo, H. Y. Hwang, *Nature* **2004**, *427*, 423.
[4] S. Thiel, G. Hammerl, A. Schmehl, C. W. Schneider, J. Mannhart, *Science* **2006**, *313*, 1942.
[5] C. Cen, S. Thiel, G. Hammerl, C. W. Schneider, K. E. Andersen, C. S. Hellberg, J. Mannhart, J. Levy, *Nat. Mater.* **2008**, *7*, 298.
[6] N. Reyren, S. Thiel, A. D. Caviglia, L. Fitting Kourkoutis, G. Hammerl, C. Richter, C. W. Schneider, T. Kopp, A. S. Rüetschi, D. Jaccard, M. Gabay, D. A. Muller, J.-M. Triscone, J. Mannhart, *Science* **2007**, *317*, 1196.
[7] A. Brinkman, M. Huijben, M. van Zalk, J. Huijben, U. Zeitler, J. C. Maan, W. G. van der Wiel, G. Rijnders, D. H. A. Blank, H. Hilgenkamp, *Nat. Mater.* **2007**, *6*, 493.
[8] D. A. Dikin, M. Mehta, C. W. Bark, C. M. Folkman, C. B. Eom, V. Chandrasekhar, *Phys. Rev. Lett.* **2011**, *107*, 056802.
[9] J. A. Bert, B. Kalisky, C. Bell, M. Kim, Y. Hikita, H. Y. Hwang, K. A. Moler, *Nat. Phys.* **2011**, *7*, 767.
[10] L. Li, C. Richter, J. Mannhart, R. C. Ashoori, *Nat. Phys.* **2011**, *7*, 762.
[11] Y. W. Xie, C. Bell, Y. Hikita, H. Y. Hwang, *Adv. Mater.* **2011**, *23*, 1744.
[12] Y. W. Xie, Y. Hikita, C. Bell, H. Y. Hwang, *Nat. Commun.* **2011**, *2*, 494.
[13] A. D. Caviglia, S. Gariglio, C. Cancellieri, B. Sacépé, A. Fête, N. Reyren, M. Gabay, A. F. Morpurgo, J.-M. Triscone, *Phys. Rev. Lett.* **2010**, *105*, 236802.
[14] C. Bell, S. Harashima, Y. Kozuka, M. Kim, B. G. Kim, Y. Hikita, and H. Y. Hwang, *Phys. Rev. Lett.* **2009**, *103*, 226802.
[15] A. D. Caviglia, S. Gariglio, N. Reyren, D. Jaccard, T. Schneider, M. Gabay, S. Thiel, G. Hammerl, J. Mannhart, J.-M. Triscone, *Nature* **2008**, *456*, 624.
[16] M. Huijben, G. Koster, H. J. A. Molegraaf, M. K. Kruize, S. Wenderich, J. E. Kleibeuker, A. McCollam, V. K. Guduru, A. Brinkman, H. Hilgenkamp, U. Zeitler, J. C. Maan, D. H. A. Blank, G. Rijnders, Preprint at http://arxiv.org/abs/1008.1896, **2010**.
[17] N. Nakagawa, H. Y. Hwang, D. A. Muller, *Nat. Mater.* **2006**, *5*, 204.
[18] Y. W. Xie, C. Bell, T. Yajima, Y. Hikita, H. Y. Hwang, *Nano Lett.* **2010**, *10*, 2588.
[19] C. Cen, S. Thiel, J. Mannhart, J. Levy, *Science* **2009**, *323*, 1026.
[20] F. Bi, D. F. Bogorin, Cheng Cen, C. W. Bark, J. W. Park, C. B. Eom, and J. Levy, *Appl. Phys. Lett.* **2010**, *97*, 173110.
[21] A. Spinelli, M. A. Torija, C. Liu, C. Jan, C. Leighton, *Phys. Rev. B* **2010**, *81*, 155110.

[22] H. P. R. Frederikse, W. R. Hosler, *Phys. Rev.* **1967**, *161*, 822.
[23] T. Ando, A. B. Fowler, F. Stern, *Rev. Mod. Phys.* **1982**, *54*, 437.
[24] G. Khalsa, A. H. MacDonald, *Phys. Rev. B* **2012**, *86*, 125121.
[25] W. Walukiewicz, H. E. Ruda, J. Lagowski, H. C. Gatos, *Phys. Rev. B* **1984**, *30*, 4571.
[26] P. Delugas, A. Filippetti, V. Fiorentini, *Phys. Rev. Lett.* **2011**, *106*, 166807.
[27] Z. S. Popović, S. Satpathy, R. M. Martin, *Phys. Rev. Lett.* **2008**, *101*, 256801.
[28] O. N. Tufte, P. W. Chapman, *Phys. Rev.* **1967**, *155*, 796.
[29] J. Son, P. Moetakef, B. Jalan, O. Bierwagen, N. J. Wright, R. Engel-Herbert, S. Stemmer, *Nat. Mater.* **2010**, *9*, 482.
[30] C. W. Schneider, S. Thiel, G. Hammerl, C. Richter, J. Mannhart, *Appl. Phys. Lett.* **2006**, *89*, 122101.

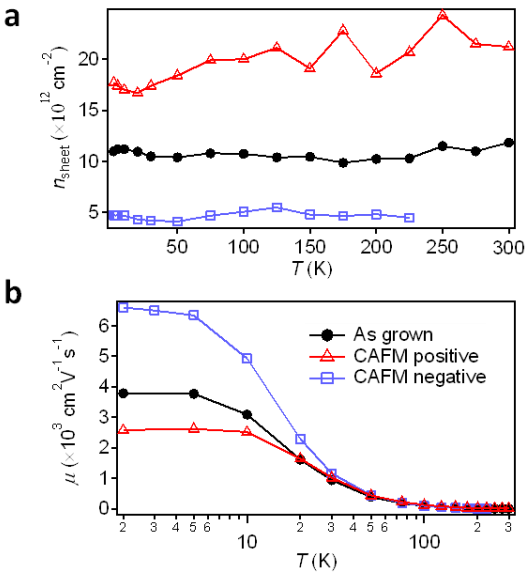

Figure 1. Tuning the interface electrons by CAFM. Temperature dependence of a) n_{sheet} and b) μ of a typical sample in as grown state (closed circles), after CAFM positive tuning (open triangles), and after CAFM negative tuning (open squares). Lines are guide for eyes. $V_{writing}$ (positive) = +8V; $V_{writing}$ (negative) = -8V. The sample was grown at 650 ˚C, with a $LaAlO_3$ thickness of 9 uc, and has been patterned into a 10 μm wide Hall bar.

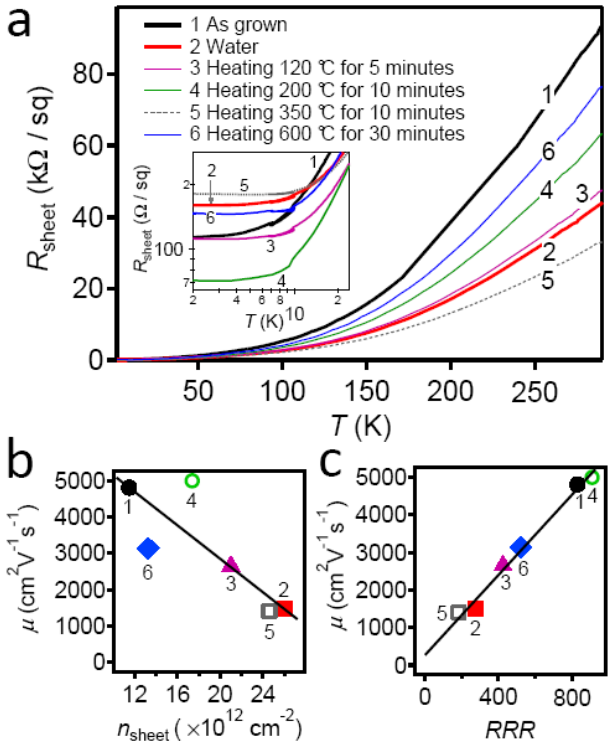

Figure 2. Tuning the charge density by water and by subsequent heating. a) R_{sheet} as a function of temperature for various conditions as indicated. The inset shows the low temperature data plotted on a log scale. b) n_{sheet} and μ measured at T = 2 K. c) μ(2K) as a function of residual resistivity ratio, *RRR*, defined as R_{sheet}(290 K)/R_{sheet}(2 K). The solid lines in b & c are guides to the eye. The sample was grown at 650 ˚C, with a $LaAlO_3$ thickness of 9 uc, and has been patterned into a 8 μm wide Hall bar. The sequence for treatments follows numerical order. The heating was performed in the growth chamber. Oxygen pressure during heating is 4 × 10^4 Pa or higher.

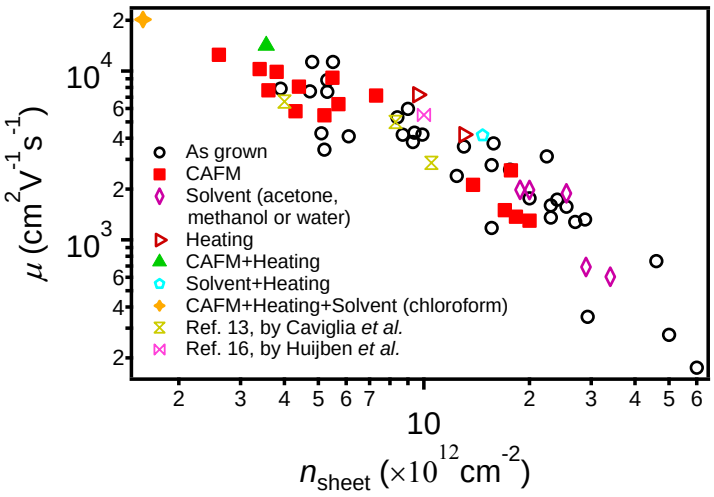

Figure 3. Summary of μ as a function of n_{sheet} for samples prepared at various conditions. The thickness of $LaAlO_3$ films varies from 5 to 10 uc. The growth temperature varies from 600 to 800 ˚C. All samples have been patterned into Hall bars whose width varies from 5 to 10 μm. For samples treated by more than one method, the sequence of the treatments is indicated in the labels. All the data were measured at T = 2 K or below.

Mobility of the electrons confined at the $LaAlO_3/SrTiO_3$ interface is significantly enhanced by surface control using surface charges and adsorbates, reaching a low temperature value more than 20,000 $cm^2V^{-1}s^{-1}$. A uniform trend that mobility increases with decreasing sheet carrier density is observed.

Keywords: Surface modification, charge transport, nanodevices, lithography

Y.W. Xie, C. Bell, Y. Hikita, S. Harashima, H. Y. Hwang

Enhancing electron mobility at the $LaAlO_3/SrTiO_3$ interface by surface control